

# Analysis on A Crossing-Fault Buried Segmented Pipeline with Flexible Joint Behaviors from Experimental Tests

**C.W. Huang**

*Chung Yuan Christian University, Taiwan*

**K.W. Chou, G.Y. Liu, L.L. Chung, C.H. Yeh, T.J. Lin & H.Y. Hung**

*National Center for Research on Earthquake Engineering, Taiwan*



**15 WCEE**  
LISBOA 2012

## SUMMARY:

Nonlinear finite element analyses considering large deformation are carried out to study the response of a segmented ductile iron pipeline that crosses a fault and undergoes normal faulting or reverse faulting. All parts of the pipeline are inter-connected with K-type joints, which are flexible joints and are widely used by water systems in Taiwan. Full-scale monotonic tensile and compression tests are conducted to better understand the mechanical behaviour of K-type joints. The joint behaviours captured from these tests are then applied in the finite element analyses. The tensile behaviour and compressive behaviour of such joints are modelled by nonlinear springs and hard contact, respectively. The soil-pipeline interaction is also carefully simulated according to the ALA-ASCE guidelines. Finally the main failure mode and failure range of a crossing-fault buried segmented pipeline are presented and discussed.

*Keywords: buried segmented pipeline, K-type joint, ductile iron pipe, soil-pipeline interaction*

## 1. INTRODUCTION

Water pipelines are vital to people. Damage of water pipelines could disrupt water supply and people daily life could be thus interrupted. Most of water pipelines are buried under the ground and strong ground motions as earthquakes can severely damage such pipelines. Past earthquakes have proved that, including Michoacán (1985), Northridge (1994), Kobe (1995), and Chi-Chi (1999).

Seismic damages on buried pipelines are contributed by permanent ground deformation (PGD) or seismic wave propagation (O'Rourke and Liu 1999). Though seismic wave propagation can damage pipelines within large geographical area, seismic PGD could cause more severe pipeline damages and such damages are often concentrated in the vicinity of the acting fault (Kim *et al.* 2010). Therefore, it could be inferred that any buried pipeline near active faults has great potential to suffer severe damage by PGD. The buried pipelines crossing known active faults would be the most vulnerable to PGD by faulting.

This study investigates the behaviour of a buried segmented pipeline that crosses a fault and suffers the most direct fault movements due to either normal faulting or reverse faulting. The commercial software, ABAQUS, is applied to carry out nonlinear finite element analysis on this pipeline given an orientation relative to the fault plane. This pipeline is considered comprising ductile iron pipes inter-connected with K-type joints, which are flexible joints. Such pipes with flexible joints are widely used by water supply systems in Taiwan. To explore the precise behaviour of this pipeline, we intend to seize the mechanical behaviour of K-type joints while the mechanical behaviour of ductile iron pipe is relatively well-known. Because it appears no study focused on such joints, several full-scale tests are conducted to investigate the mechanical behaviour of K-type joints. Axial tensile and compression tests on segmented pipelines are developed to determine the tensile and compressive behaviours of K-type joints.

In pipeline analyses, the finite element method (FEM) is widely used because it can consistently account for the nonlinear stress-strain response of the pipeline, the longitudinal and transverse soil resistance, and second-order effects induced by large displacements. Numerical simulation also has another advantage—it shows no limits on simulating the pipelines that occupy vast space. In this study, the responses of buried segmented pipelines subjected to normal and reverse fault movements are investigated by solid-mode finite element analysis (ABAQUS 2011). The interactions between soil and pipelines are modelled by nonlinear soil springs. More importantly, the mechanical behaviours of K-type joints captured from the tensile and compression tests are taken into account in the finite element analyses. The tensile behaviours of K-type joints are modelled by nonlinear springs while the compressive behaviours get elicited by activating hard contacts in the finite element analysis. Through such finite element simulation, the main failure mode and failure range of the buried segmented pipelines under normal and reverse fault movements are presented and discussed.

## 2. TESTS ON K-TYPE JOINT BEHAVIOR

Several tests are carried out to explore the tensile and compressive behaviour of K-type joints. In each test, the studied specimen is a segmented pipeline comprising two ductile iron pipes that are connected with a K-type joint. One ductile iron pipe (DIP) acts as the spigot, and the other as the socket. All DIPs in these tests are either 200 mm or 400 mm in diameter. The tensile and compression tests on mechanical behaviours of K-type joints are described in the following.

### 2.1 Joint Tensile Test

Two different sizes of DIPs with K-type joints, 200 or 400 mm in diameter, are used in these tests. The two DIPs are 6 m in length, the general length of DIPs made in Taiwan. Each DIP is cut into two 3m pipes. As aforementioned, one is the spigot, retaining the spigot end of the uncut DIP, and the other is the socket, which retains the socket end of the uncut. As expected, the spigot may be inserted and fitted into the socket. The insertion length follows the regulation of CNS10808-G3219. Before being inserted into the socket, the non-spigot end of the spigot is fastened to the actuator, and the non-socket end of the socket is attached to the reaction wall (See Fig. 1). Around the vicinity of the joint, a steel frame is fitted to prevent the jointed pipeline from large flexural deformation caused by the weight of this pipeline.

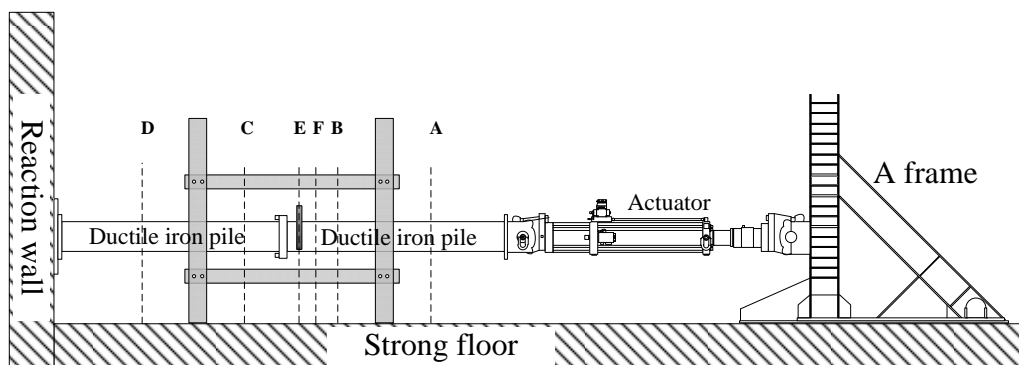


**Figure 1.** The assembly in tensile tests

#### 2.1.1 Joint displacement measurement

The movement and output force of the actuator is recorded throughout. Additionally, a displacement meter is attached to the jointed pipeline to measure the joint relative displacement, and a NDI optical measurement system is setup to make sure the meter gets correct displacement measurement. Fig. 2 shows how the meter and the NDI system are installed: the meter is secured across the joint, along the axial direction of the pipeline, and the NDI system has four LED markers glued onto the pipe surface around the joint. Because the NDI system can capture the displacement of LED markers, two markers

are placed on the spigot and the socket pipes respectively so that the joint relative displacement can be approximated as the difference between the NDI-captured displacements of two markers adjacent to the joint, one marker on the spigot side and the other on the socket side.

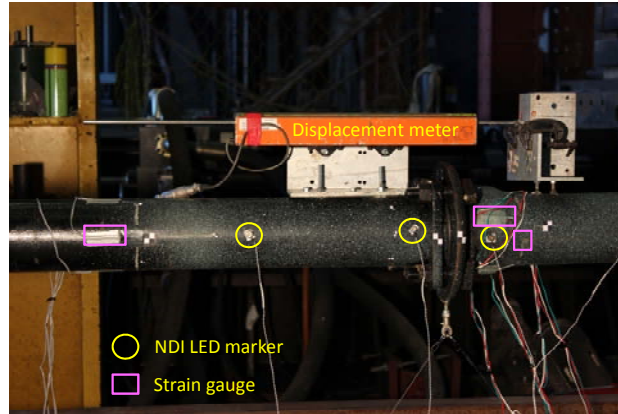


**Figure 2.** The displacement meter, strain gauges, and NDI LED markers

### 2.1.2 Actuator force vs. displacement

Fig. 3 shows the actuator’s force-displacement relationships in tensile tests on the diameter-200 mm pipe and diameter-400 mm pipe. Exp1, Exp2, and Exp3 denote three different tests on the same pipe specimen. For the diameter-200 mm pipe tests, the maximum force, 48.0 kN, occurs in the Exp1 test. For 400 mm, the maximum force 90.5 kN appears in the Exp3. Table 1 shows the two maximums are far less than their corresponding pipe axial yield forces (the yield stress of DIPs is supposed to be 450 MPa). In summary, during any tensile test, the actuator force never makes any DIP yield even when a DIP is pull out from the K-type joint. Because the actuator force balances the friction the joint offers before the pull-out, the maximum actuator force is defined as the joint tensile strength as shown in Table1. Therefore, it could be concluded that the joint tensile strength or the actuator force maximum, is considerably insufficient for the joint to keep connecting the socket with spigot until any DIP begins to yield.

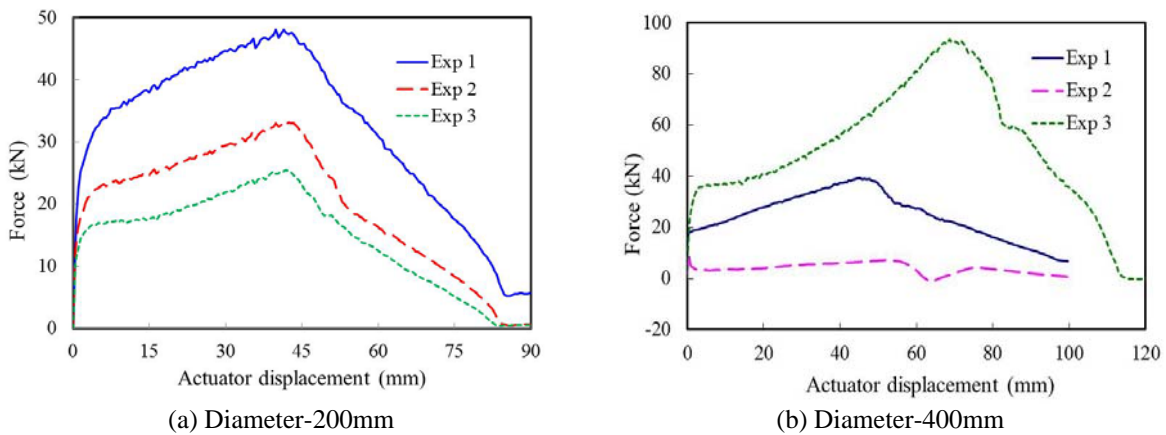


**Figure 3.** Actuator force vs. displacement in tensile tests of K-type joint

**Table 1.** Cross-section properties and joint tensile strengths

Diameter (mm)	Section Area (mm <sup>2</sup> )	Yield axial force (kN)	Ultimate axial force (kN)	Joint tensile strength (kN)
200	4033.80	1270.65	1815.21	48.0
400	9205.49	2899.73	4142.47	90.5

Though on the same pipeline, the load-displacement curves of Exp1, Exp2, and Exp3 are clearly different. This indicates the same joint produces different histories of friction against the actuator in these three tests. Since such friction is developed between the pipe wall and the rubber ring, this test outcome could be interpreted by how the rubber ring is installed and how it acts on the same pipe wall in different tests.

First, a rubber ring must be manually lubricated before installed around the head of the spigot. Since it is almost impossible to be lubricated equally in every test, a rubber ring could not get identically tightened after it is installed on the spigot. Thus a rubber ring with the same pair of socket and spigot could generate different friction histories in different tests.

The tendencies of almost all the actuator force-displacement curves appear similar in these tests. The actuator first overcomes the static friction, then the kinetic friction. The kinetic friction goes up along with increasing tensile displacement. But once the tensile displacement exceeds the installation length, the kinetic friction starts decreasing because the contact area where the friction is generated turns smaller and smaller.

### 2.1.3 Pipe as rigid body in tension

Fig. 4 helps us compare displacement time series from the actuator, displacement meter, and NDI system. In each tensile test, the actuator displacement series matches the displacement meter series, which approximates the time series of the joint relative displacement. So the actuator displacement approximates the joint relative displacement. On the other hand, the actuator displacement is equal to the summation of the joint relative displacement and the total of the axial deformations of the socket and spigot. Since the actuator displacement approximates the joint relative displacement, the axial deformation total is quite little and considered insignificant. In other words, the jointed pipeline suffers almost no axial deformation. It behaves as a rigid body during the tensile tests. This inference could be verified with what the strain gauges measure.

Four uniaxial strain gages are glued onto the pipe surface at cross section A, B, C, and D shown in Fig. 1, respectively. Four triaxial strain gages, adjacent to the joint, glued onto the pipe surface at cross section F. Their readings are within the range of  $\pm 10^{-5}$ , a clear indication that the socket and spigot suffer almost no deformation while the reading resolution of the uniaxial gages is  $2\% \times 10^{-6}$  and that of the tri-axial is  $5\% \times 10^{-6}$ .

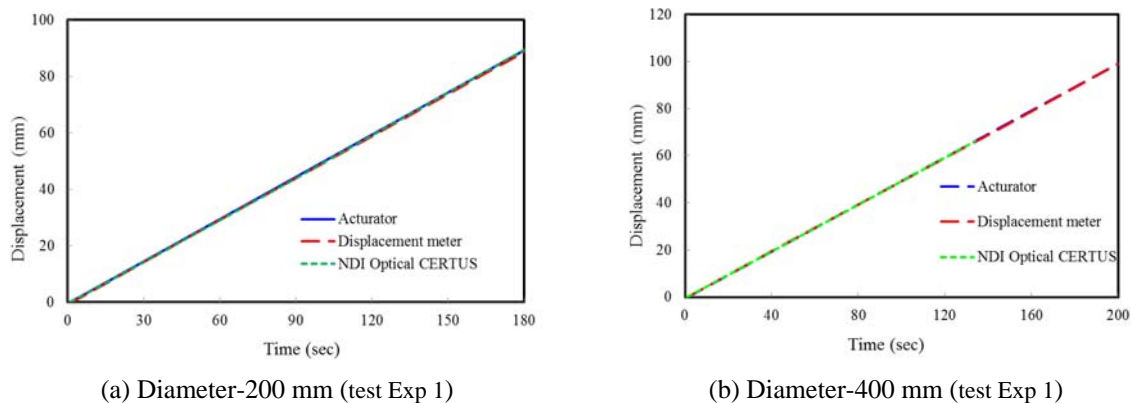


**Figure 4.** Displacement time series measured in “Exp 1” tensile tests

## 2.2 Joint Compression Test

Under compression, the jointed pipeline would buckle fairly early if the spigot or the socket is 3 m long as in the tensile tests. If that’s the case, the pipeline or the joint could fail to reach its compressive strength at the end of the test, i.e. the time the actuator stops compressing the buckling pipeline. So in the compression test, the length of the spigot and the socket is changed to twice the diameter of the

pipeline. Besides, this pipeline is subjected to a 500-ton universal testing machine in NCREE (See Fig. 5), while the 100-ton actuator in tensile tests could be incapable of eliciting any form of failure from the pipeline above 200 mm in diameter.



**Figure 5.** The 500-ton universal testing machine in joint compression tests

Fig. 6 shows there are two displacement meters to measure the joint displacement. As in the tensile tests, a NDI optical measurement system is also setup to ensure that correct measurements on the joint relative displacement are obtained in the compression tests. The spigot and the socket have two NDI-required markers respectively.



**Figure 6.** The displacement meters and NDI markers from C1 to C4

In Fig. 7,  $P_y$  denotes the axial compressive yield strength of the DIPs participating in the compression tests, and  $P_u$  denotes the axial compressive ultimate strength. For the diameter-200 mm pipeline, at first, the actuator force increases linearly with displacement. After reaching  $P_y$ , the force increasing slows down until reaching a peak greater than  $P_u$ . For the diameter-400 mm pipeline, the actuator force also increases linearly before reaches  $P_y$ . But after  $P_y$ , a plateau is developed where the displacement keeps on increasing but the force appears unchanged. The actuator force drops after the plateau and never reaches  $P_u$ .

In the compression tests, All DIPs were yielded. The diameter-200 mm DIPs even experienced their compressive ultimate strength. All the jointed pipelines buckled and right after that, the actuator stops compressing them. The buckling occurred around the tops of these pipelines, where they were connected with the actuator (See Fig. 6). In contrast, during the whole process, all K-type joints had no visible deformation. No failure of the K-type joints was observed when those DIPs reached their  $P_y$  or even the  $P_u$ .

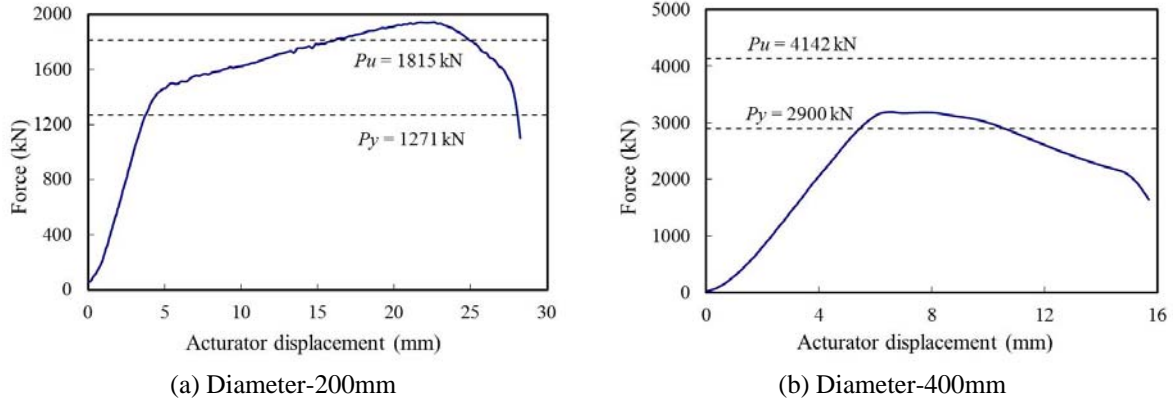


**Figure 7.** Actuator force vs. displacement in compression tests on K-type joints

### 3. CROSSING-FAULT SEGMENTED PIPELINE SIMULATION

The responses of segmented ductile iron pipelines under normal faulting or reverse faulting are studied by using the commercial finite element program ABAQUS (2011). Soil movement along the fault plane causes soil-pipeline interaction in three dimensions. In finite element analysis, such soil-pipeline interaction is modelled by discrete nonlinear soil springs (SPRING2 in ABAQUS), and the force-displacement relationships of these springs are described by ASCE-ALA (2005). In addition, the segmented pipelines are modelled by solid elements (C3D8I in ABAQUS). Each node of these solid elements is connected with a soil spring that has stiffness in the axial, transverse horizontal and transverse vertical directions. Such a soil spring has two ends. One is connected with a node of a solid element, the other a ground node. Before the fault moves, the position of this ground node is the same as that of the solid element node with which the soil spring is connected. Such ground nodes are prescribed with displacements consistent with the fault movement. Besides, geometric and material nonlinearities of the ductile iron pipelines are taken into account, which are requisite for resolving the pipeline large deformation caused by faulting.

The ALA-ASCE guidelines (2005) define the longitudinal, transverse horizontal, and transverse vertical soil springs with three bilinear load-deformation curves (See Fig. 8). Each load-deformation curve is described by maximum soil resistance to the pipe and a corresponding soil displacement. It is worth emphasizing that such resistance is given in force per unit length of pipe and can be directly applied to beam elements. Nevertheless, the maximum soil resistance needs to be transformed to equivalent soil spring forces that can be applied to nodes of the pipeline that is modelled by solid elements. First, the soil resistance is transformed to soil pressure that may be applied uniformly to the pipeline surface. In the longitudinal direction, the soil pressure can be obtained by dividing the resistance by the outer circumference of the pipeline cross section. In directions of transverse vertical and transverse horizontal, the soil pressure depends on the nodal coordinates relative to the center of the cross section (Palmer *et al.* 2009). The soil pressure in the three directions can be calculated from Eqn. (4.1), and the corresponding distribution is shown in Fig. 9.

$$\bar{p}_t = t / (\pi D) \quad (4.1 \text{ a})$$

$$\bar{p}_p(\varphi) = (2p)(1 - \cos 2\varphi) / (\pi D) \quad (4.1 \text{ b})$$

$$\bar{p}_{q_d}(\theta) = (2q_d)(1 - \cos 2\theta) / (\pi D) \quad (4.1 \text{ c})$$

$$\bar{p}_{q_u}(\theta) = (2q_u)(1 - \cos 2\theta) / (\pi D) \quad (4.1 \text{ d})$$

where  $D$  is the outer diameter of the pipeline. In addition,  $t$ ,  $p$ ,  $q_u$ , and  $q_d$  represent the soil resistance to the pipe and can be calculated according to ALA-ASCE guidelines (2005). After the soil pressure is

obtained, the equivalent spring forces can be calculated by following the computation of equivalent nodal forces in the finite element method.

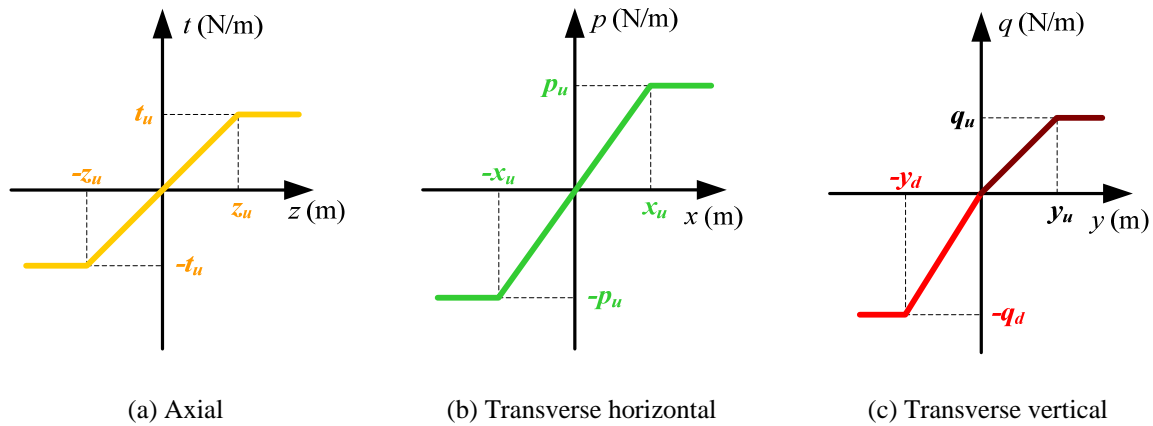


**Figure 8.** Soil spring load-deformation relationships

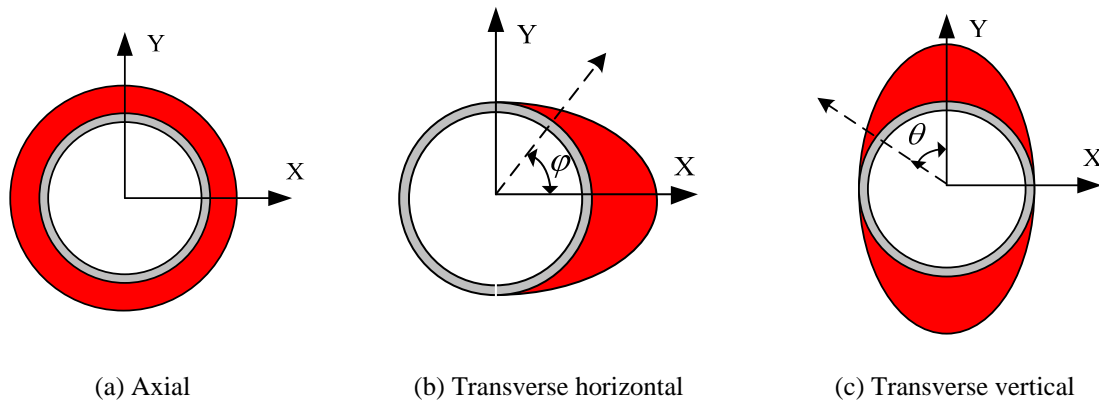


**Figure 9.** Soil pressure distributions

Every DIP of the pipeline is connected with another DIP through a K-type joint. The mechanical behaviour of a K-type joint is modelled by nonlinear translational springs and rotational springs. It is worth emphasizing that the tensile behaviour of K-type joints captured from the tensile tests is further approximated by a piecewise linear force-displacement relationship (See Fig. 10(a)). This relationship is then applied to define the behaviour of those translational springs. In contrast, the compressive behaviour of K-type joints is modelled by “hard contact” in finite element analysis. Though the complete compressive behaviour of K-type joints cannot be captured from the compression tests, any K-type joint under compression is considered strong enough to sustain connecting two DIPs even if they are buckling; because no visible deformation were shown on the K-type joints in the compression tests.

In the transverse direction, the stiffness of a K-type joint is considered much larger than the stiffness in the longitudinal direction. Thus the stiffness in the transverse direction is assumed to be ten times the initial slope of the actuator force-displacement relationship from a joint compression test. Besides, the moment-rotation relationship of a K-type joint is obtained from finite element simulation of this joint (Huang *et al.* 2012). The moment-rotation relationship also get further approximated by a piecewise linear curve, as shown in Fig. 10(b). Then this curve is used to define the joint-equivalent nonlinear rotational springs.

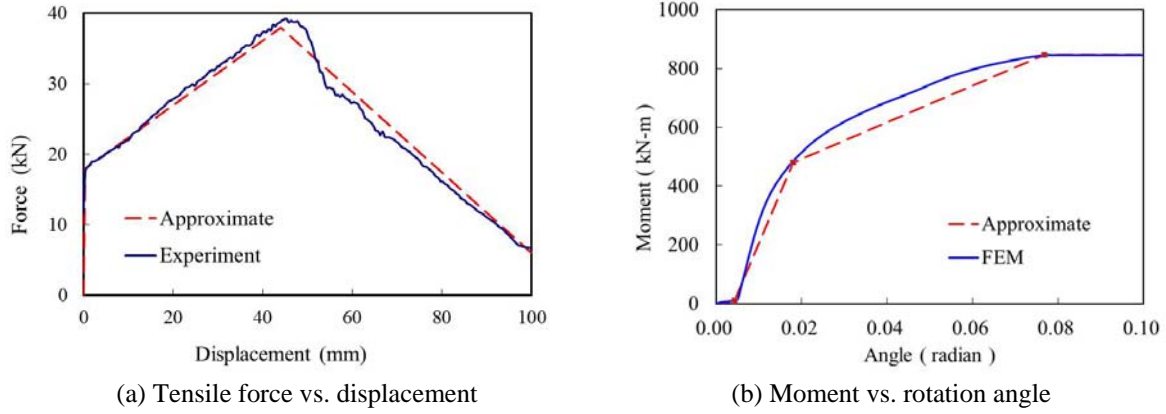


**Figure 10.** The generalized behaviours of joint-equivalent springs

In finite element analysis, every DIP is 6 m in length, having a cross section of which the external diameter ( $D$ ) is 0.426 m and the wall thickness is 0.007 m. The length of the pipeline comprising all DIPs is 36 m (90 times the pipe diameter) to keep the ends of the pipeline from boundary effects. The geometric relationship between the pipeline and the fault plane is depicted in Fig. 11 where the axis X, Y, and Z denote the transverse horizontal, transverse vertical, and longitudinal directions of the pipeline. The fault plane crosses the middle point of the pipeline. The plane intersects the pipeline axis with an angle  $\alpha$  ( $\alpha = 30^\circ$ ) in the YZ plane and with an angle  $\beta$  ( $\beta = 90^\circ$ ) in the XZ plane. The right half of the pipeline (including the end nodes of the pipeline) remains fixed during fault movement, as located in the footwall for the fault. In the left of the fault plane, or in the hanging wall, all ground nodes are imposed with displacement consistent with fault movement. The pipeline is discretized by 40 solid elements around the cylinder circumference, while the size of the solid element in the longitudinal direction is chosen as 1/100 of the length of a DIP.

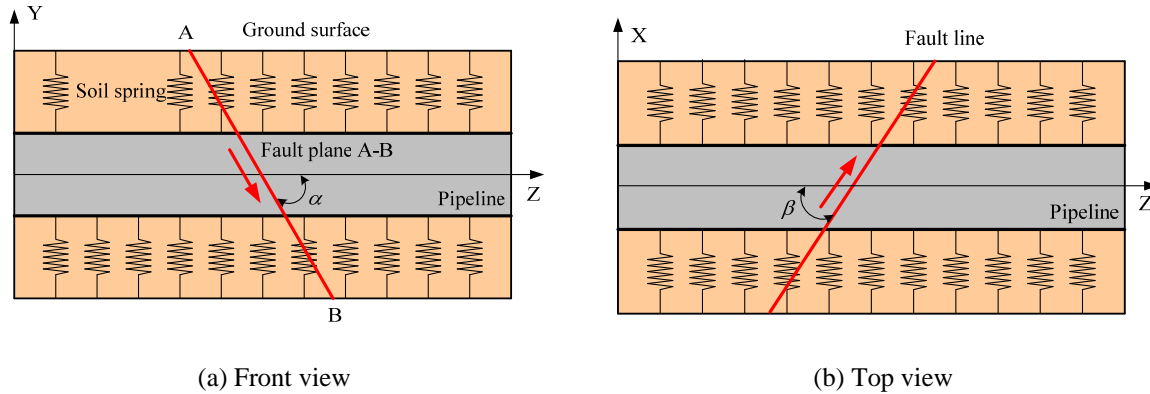


**Figure 11.** The geometric relationship between the fault and the buried pipeline

The stress-strain relationship of DIPs is simply described by three consecutive linear relationships. The initial elastic modulus is 170 GPa and the Poisson's ratio is 0.3. The yield stress is 315 MPa and the post-yield modulus ratio is 0.03 (5.1 GPa). After the post-yield stress (560 MPa), which corresponds to 5% strain, the stress-strain relationship becomes perfectly plastic.

The pipeline lies within soil. The center of the pipeline is assumed to be 1.5m under the ground. The underground soil is made of only dense silty sand with friction angle  $\phi = 35^\circ$  and effective unit weight  $\gamma = 16.6 \text{ kN/m}^3$ . The coefficient of friction between the pipeline surface and the surrounding soil is considered 0.7. The native soil and the backfill soil are assumed to have the same mechanical properties. Besides, the nonlinear analyses are carried out in a displacement-controlled scheme that gradually increases the fault movement  $\Delta$ . At each increment of fault movement, stresses and strains of the pipeline and the equivalent forces from soil springs are recorded.

Fig. 12(a) shows that the effective stress contour at the central of the pipeline in its deformed shape under normal fault movement  $\Delta = 0.5\text{m}$ . One can also observe a local stress concentration at the middle joint of the pipeline where the fault plane crosses the pipeline. Nevertheless, the main failure mode of the segmented pipeline is the pull-out of the DIPs at all the K-type joints in the hanging wall. The maximum separation of these DIPs occurs at the K-type joint that is the closest to the left end of the pipeline. Away from this joint, the leftmost DIP is completely pulled out (See Fig. 12(b)) because no further restraint is applied to the left end of the left most DIP. In fact, all the DIPs in the left hand side of the fault plane (or in the hanging wall) have different degrees of tensile separation at K-type joints. These separations could cause leakage from the segmented pipeline.

Figures 12(c) shows that the effective stress contour at the central of a pipeline in its deformed shape under reverse fault movement  $\Delta = -0.5\text{m}$ . The maximum effective stress occurs at the middle point of the pipeline where the fault plane crosses the pipeline. One can observe the local buckling at the central K-type joints of the pipeline under reverse fault movement. At the right part of the pipeline, the K-type joint next to the central joint also failed with local buckling shown in Figure 12(d).

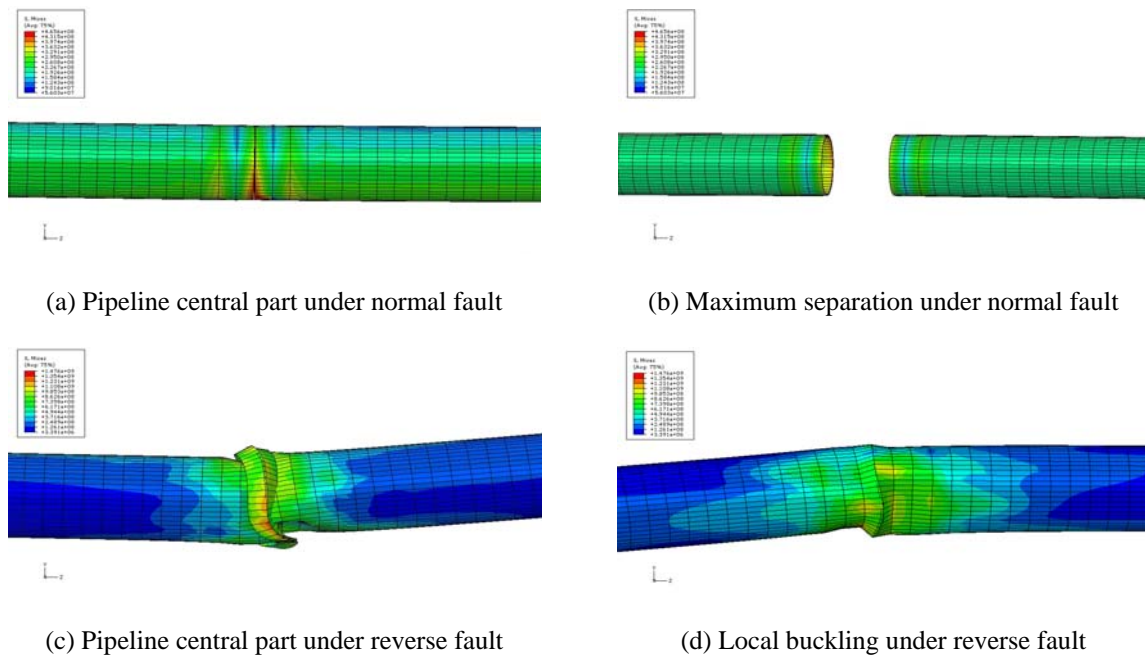


**Figure 12.** The effective stress contours at the middle K-type joint under different fault movements

#### 4. CONCLUSIONS

The tensile behaviour of K-type joints is found out in the tensile tests. From a K-type joint, a ductile iron pipe can be pulled out by the actuator using a pulling force far less than the tensile strength of that pipe. During the whole pulling process, all the tested pipes suffer little stress and strain, behaving as rigid bodies. On the other hand, the compression tests fail to find out the actual compressive strength of the K-type joints. Although the jointed pipelines undergo buckling, these joints have no visible deformation and are able to sustain connection between ductile iron pipes through the whole compression tests.

Subjected to normal fault movement in finite element analysis, the segmented pipeline fails because its ductile iron pipes in the hanging wall are pulled out from K-type joints. The pipe farthest to the fault plane gets the maximum pull-out. Therefore, for a crossing-fault pipeline, its failure range could cover all the pipes in the hanging wall. The corresponding pipe separations at joints would cause severe water leakage if this pipeline undergoes extensive faulting-caused permanent ground deformation.

Under reverse fault movement in finite element analysis, the segmented pipeline fails because of the occurrence of local buckling around several K-type joints. Such buckling failures are concentrated around two K-type joints near the fault plane. One is the central joint (or the middle point) of the pipeline where the pipeline crosses the fault plane. The other is in the footing wall and next to the central joint.

#### **ACKNOWLEDGEMENT**

This study was funded by Water Resources Agency, Ministry of Economic Affairs, Taiwan, under Contract No. MOEA-WRA-1000090 and No. MOEA-WRA-1010381. We are also grateful to Simutech Solution Corporation (Taiwan) for providing computational resources.

#### **REFERENCES**

- ABAQUS version 6.10 (2011). Analysis Users Manual, Dassault Systèmes Simulia Corporation, Providence RI, USA.
- American Lifelines Alliance (2001), Guidelines for the design of buried steel pipe (with addenda through February 2005), American Society of Civil Engineering (ASCE), USA.
- Huang, C. W., Hsu, H. W., Liu, G. Y. and Chung, L. L. (2012). Experimental validation and numerical simulation on the mechanical behaviors of K-type joints. *International Journal of Pressure Vessels and Piping*. (In preparation).
- Kim, J., Lynch, J. P., Michalowski, R., Green, R.A., Pour-Ghaz, M., Weiss, W.J., and Bradshaw, A. (2009). Experimental study on the behavior of segmented buried concrete pipelines subjected to ground movements. *Proceedings of the 16th Annual International Symposium of SPIE Smart Structures/NDE*. Vol 7294.
- O'Rourke, M. J. and Liu, X. (1999). Response of Buried Pipelines Subject to Earthquake Effects, Multidisciplinary Center for Earthquake Engineering Research, University at Buffalo, USA.
- Palmer, M. C., O'Rourke, T. D., Olson, N. A., Abdoun, T. H., Ha, D. and O'Rourke, M. J. (2009). Tactile pressure sensors for soil-structure interaction assessment. *Journal of Geotechnical and Geoenvironmental Engineering* **135**: 11,1638-1645.